Hindawi Publishing Corporation
Mathematical Problems in Engineering
Volume 2014, Article ID 594962, 15 pages
http://dx.doi.org/10.1155/2014/594962

Research Article

Spontaneous Synchronization in Two Mutually Coupled Memristor-Based Chua's Circuits: Numerical Investigations

Eleonora Bilotta, Francesco Chiaravalloti, and Pietro Pantano

Department of Physics, University of Calabria, Via Pietro Bucci, 87036 Arcavacata di Rende (CS), Italy

Correspondence should be addressed to Francesco Chiaravalloti; francesco.chiaravalloti@unical.it

Received 11 December 2013; Revised 27 March 2014; Accepted 27 March 2014; Published 7 May 2014

Academic Editor: Hamid Reza Karimi

Chaotic dynamics of numerous memristor-based circuits is widely reported in literature. Recently, some works have appeared which study the problem of synchronization control of these systems in a master-slave configuration. In the present paper, the spontaneous dynamic behavior of two chaotic memristor-based Chua's circuits, mutually interacting through a coupling resistance, was studied via computer simulations in order to study possible self-organized synchronization phenomena. The used memristor is a flux controlled memristor with a cubic nonlinearity, and it can be regarded as a time-varying memductance. The memristor, in effect, retains memory of its past dynamic and any difference in the initial conditions of the two circuits results in different values of the corresponding memductances. In this sense, due to the memory effect of the memristor, even if coupled circuits have the same parameters they do not constitute two completely identical chaotic oscillators. As is known, for nonidentical chaotic systems, in addition to complete synchronizations (CS) other weaker forms of synchronization which provide correlations between the signals of the two systems can also occur. Depending on initial conditions and coupling strength, both chaotic and nonchaotic synchronization are observed for the system considered in this work.

1. Introduction

One of the most important topics of contemporary science focuses on the study of continuous and discrete dynamical systems [1–3], analysing their organization as nonlinear evolving structures [4–6] or as artificial agents in synthetic environments [7, 8]. Chaos is the most striking feature of their behaviour. Chaotic systems are nonlinear deterministic systems that display highly complex dynamic with several peculiar features such as fractal properties of the motion in the phase space (strange attractors) and, especially, extraordinary sensitivity to initial conditions and system parameters variations. This implies that, even for two identical chaotic systems, a slight difference in the initial conditions grows exponentially in time resulting in completely different trajectories. Consequently, chaotic systems intrinsically would seem to defy synchronization. Nonetheless, two coupled chaotic systems also can exhibit some form of synchronization, meaning by that a dynamical state wherein a correlation exists among a given property of their motion [9, 10].

The synchronization between chaotic systems, either identical or nonidentical, is a fundamental phenomenon in nonlinear dynamics, observed in diverse areas of science and technology. Studies on chaos synchronization are of great interest, both from a theoretical and applicative point of view, due to their possible applications, for example, in cryptography and secure communications [11–13]. The synchronization of chaotic oscillators is also an important process in many biological systems [14].

Since the pioneering works of Pecora et al. [9, 15], it has become known that it is possible to force two chaotic systems to synchronize, and various methods for chaos control and synchronization have been developed [16] such as those based, for example, on sliding-mode control or linear matrix inequality, just to name a few [17–21].

On the other hand, spontaneous synchronization is also possible for nonlinear systems. More precisely, depending on the modalities of interaction between the systems, it is possible to distinguish between two configurations leading to synchronization: unidirectional coupling (drive-response or master-slave configuration) and bidirectional coupling [10, 22].

In the first case, one of the two systems evolves freely and forces the other system to follow a certain function of the master dynamic, producing external synchronization. This approach is affected, in large part, by the point of view of the dynamics systems control theory. For example, the synchronization control of memristor-based chaotic systems in a drive-response configuration has been recently studied using adaptive control and fuzzy modelling [23, 24].

On the contrary, in the bidirectional coupling configuration spontaneous synchronization is due to the mutual interactions between the chaotic oscillators which self-organize their dynamics and, in this case, the synchronization is configured as an emergent phenomenon. In effect, spontaneous synchronization is recognized in various areas, ranging from physics to biology and social sciences [25]. A typical bidirectional coupling producing synchronization for many dynamical systems is the so-called "diffusive coupling," where the mutually forcing term is proportional to the differences between the states of the systems [26, 27]. The present work considers this coupling configuration and, for the first time as far as the authors' knowledge is concerned, results of numerical investigations on the spontaneous dynamics of two resistively coupled memristor-based Chua's circuit are presented. The "memristor" is the so-called fourth elementary circuit element, theorized by Chua in 1971 [28] in order to complete the mathematical relations connecting pairs of the four fundamental circuit variables (current, voltage, charge, and magnetic flux). It is a two-terminal circuit element in which the magnetic flux φ between the terminals is a nonlinear function of the electric charge q that passes through the device. Formally, a memristor is characterized by a relation $f(\varphi, q) = 0$, called "the memristor constitutive relation," linking charge and flux, and its memductance is defined as $W(\varphi) = dq(\varphi)/d\varphi$. In the case of nonlinear constitutive relation, the memductance value depends upon the history of the device (i.e., taking into account the Lenz's law $V = d\varphi/dt$, the memductance varies according to the integral over time of the applied voltage). Therefore, the behavior of the memristor depends on its past history and the memristor retains memory of its state even when no current passes through it.

Despite its theorization in 1971, a physical realization of a memristor only occurred in 2008 in the form of a nanometer-sized solid-state two-terminal device, realized by Stan William's group at the Hewlett-Packard (HP) Labs [29]. After its discovery, studies on the special properties of the memristor as electric device have received increasing interest [30, 31]. Many papers focus on the possible technological applications of the memristor, for example, in order to build ultra-dense nonvolatile memories [32], or new kinds of high performance computers [33, 34]. Moreover, the special properties of the memristor appear useful in the modelling cognitive process [35, 36] and to emulate the human brain [37, 38]. The memristor is also of great interest in the field of chaotic dynamical systems. Due to the nonlinearity of its constitutive relation, the memristor-based circuits can generate chaotic dynamics [39–44]. In particular, depending on the parameters and initial conditions of the memristor, a chaotic circuit with memory can produce transient chaos and intermittence [45–47].

The memristor used in this work is characterized by a cubic nonlinearity that makes the behavior of the single circuit chaotic. Since the actual memductance value depends on the history of the applied voltage, starting from different initial conditions the memristors in the two circuits have different memories, which results in different values of the memductance. In this sense, despite having the same circuit parameters, the two circuits can be viewed as nonperfectly identical chaotic oscillators.

It is worth noting that for nonequivalent chaotic oscillators, and depending on the coupling strength, several kinds of synchronization exist [10, 15, 48]. In particular, for identical systems complete synchronization (CS) is possible, and the trajectories of the two systems overlap perfectly. For example, it is known that two bidirectional coupled Chua's circuit reach a state of complete synchronization [49]. A weaker form of synchronization, also possible for nonidentical systems, is phase synchronization (PS), where only the phases of the interacting oscillators are correlated [50]. Other forms of synchronization are lag synchronizations (LG) [51, 52] and rhythm synchronization (RS) [53], characterized by a fixed time lag between the trajectories of two coupled nonidentical oscillators. A more general synchronization state, that seems to be the chaos synchrony most frequently found in natural systems [54], is the generalized synchronization (GS). It is characterized by a functional relationship between the trajectories of two coupled systems [55, 56], either identical or nonidentical. Therefore, generally speaking, chaos synchronization refers to a dynamic process in which two coupled chaotic systems adjust a given property of their motion to a common behavior, ranging from complete agreement of trajectories to a generic relationship between them.

In order to evaluate the presence of synchronization, the two-dimensional phase portrait between corresponding signals can be used. When CS occurs, the phase portrait consists in a straight line at 45°. Conversely, if two signals are uncorrelated there will be an isotropic cloud of points in the diagram. Between these two extremes, any "structure" in the phase diagram indicates the existence of some kind of correlation between the signals.

In this work, synchronization states, in the sense discussed above, were identified by the appearance of patterns in the phase portraits. This paper is organized as follows. In Section 2, the single memristor based Chua's circuit is presented. The diffusive coupling schema and the equations for the coupled circuits are derived in Section 3. Results of numerical simulations are presented in Section 4. Finally our main conclusions are summarized in Section 5.

2. The Memristor-Based Chua's Circuit

The memristor-based chaotic circuit considered in this work was proposed and described by Muthuswamy [57]. It consists

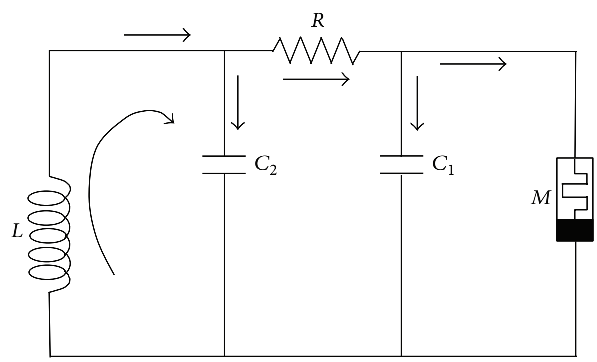

Figure 1: The memristor-based Chua's circuit: the Chua's diode is replaced by a flux-controlled active memristor.

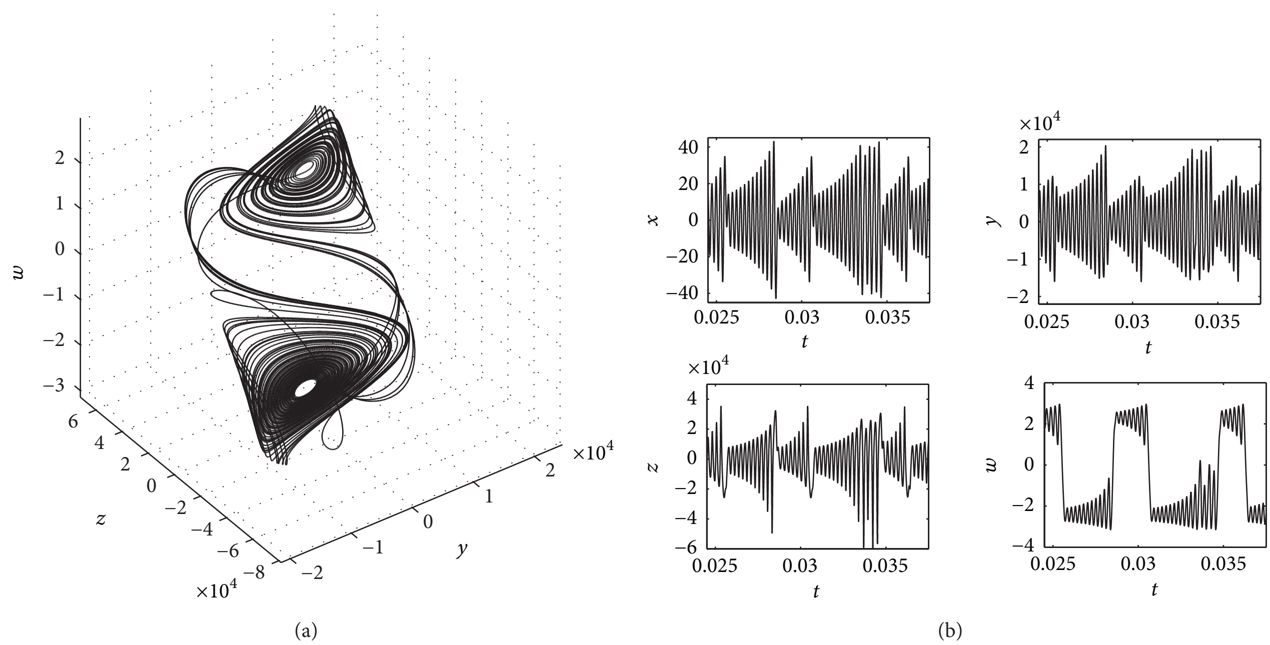

Figure 2: 3D projection of the double-scroll type attractor generated by (3a)–(3d) for initial conditions [−24.33, −12480, −7294, 2.948] and corresponding state variables x, y, z, and w as a function of the time.

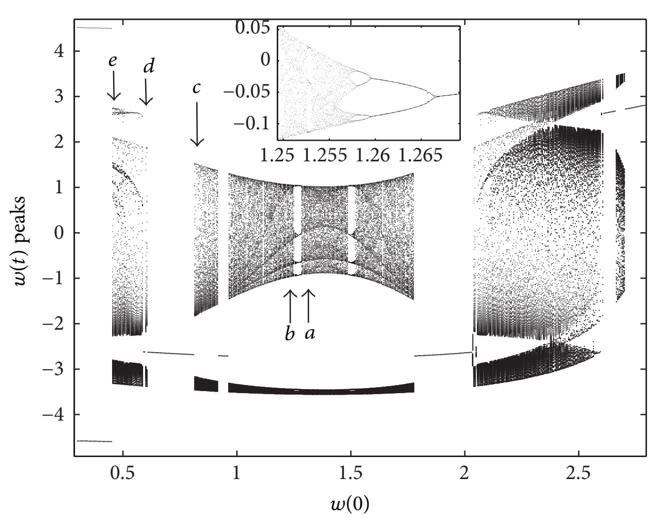

Figure 3: Peaks of the signal $w(t)$ vs $w(0)$ for initial conditions [0, 23000, 1250, $w(0)$]. The arrows indicate progression of the dynamics described in the text. The zoom-in at the top shows a particular of the map with a period doubling scenario.

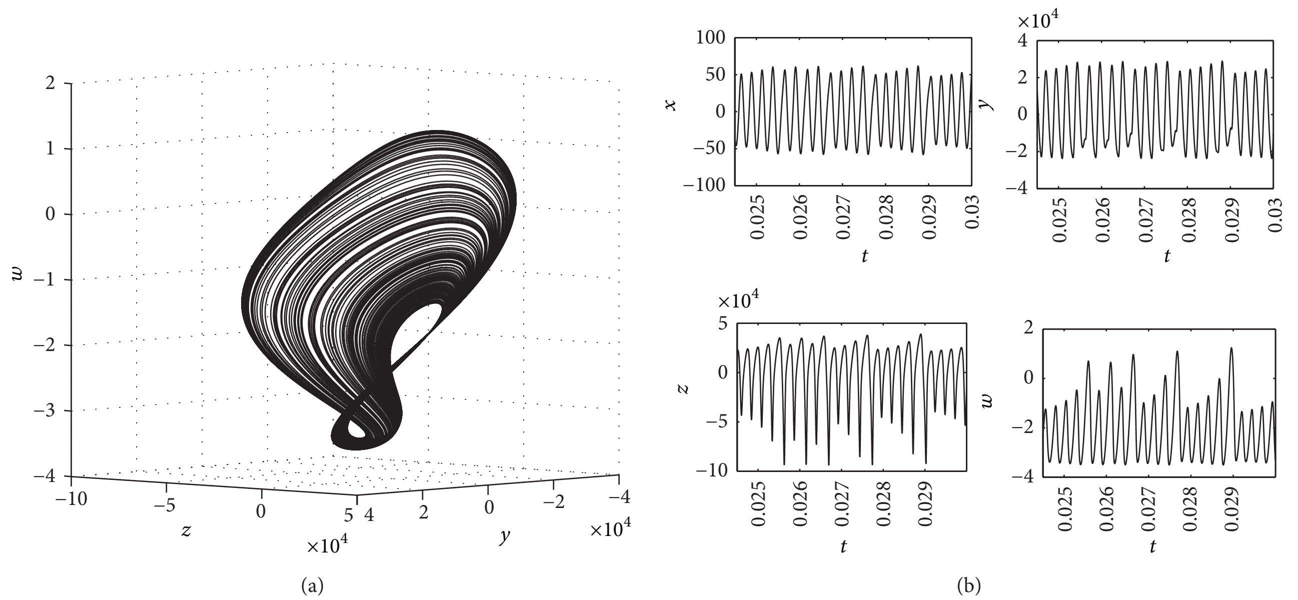

Figure 4: 3D projection of the Chua's spiral-type attractor generated by (3a)–(3d) for initial conditions $[0.0\ \ 23000\ \ 1250\ \ 1]$, and corresponding time series of state variables x, y, z, and w.

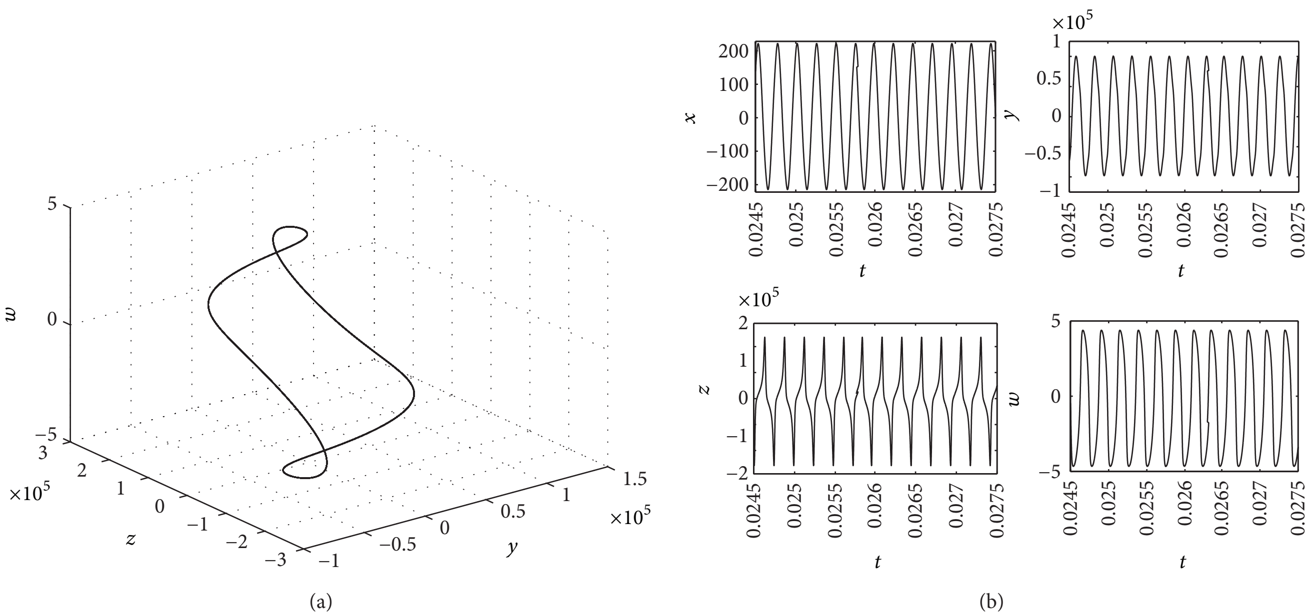

Figure 5: 3D projection of the one-period limit cycle attractor generated by (3a)–(3d) for initial conditions [112.4047, 27015, 9360, −4.0542], and corresponding nonchaotic pseudosinusoidal oscillations of higher amplitude with respect to the chaotic dynamic.

of a Chua's circuit with the diode replaced by a flux-controlled active memristor (Figure 1) characterized by a cubic continuous nonlinearity for the $q - \varphi$ constitutive relation:

$$q(\varphi) = \alpha\varphi + \beta\varphi^3, \quad (1)$$

where $\alpha = -0.667 \cdot 10^{-3}$ and $\beta = 0.029 \cdot 10^{-3}$. The memductance is given by

$$W(\varphi) = \alpha + 3\beta\varphi^2. \quad (2)$$

Note that the memductance is negative for $\varphi \in (-\sqrt{-\alpha/(3\beta)}, \sqrt{-\alpha/(3\beta)})$, therefore the considered memristor is an active element on this interval of magnetic flux [39, 57].

By applying the Kirchhoff's laws to the memristor-based Chua's circuit of Figure 1, the following state equations are obtained:

$$\frac{dx}{dt} = -\frac{y}{L}, \quad (3a)$$

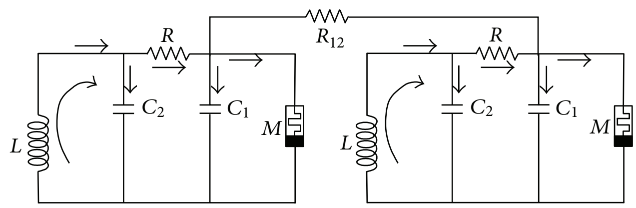

Figure 6: The system of two memristor-based Chua's circuits bidirectionally coupled via a resistor.

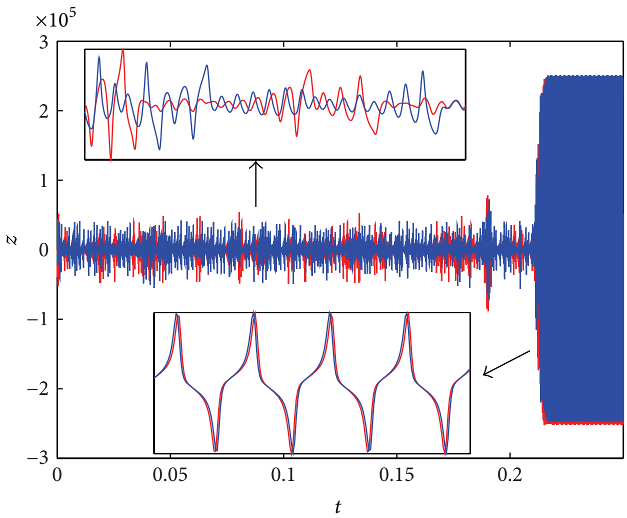

Figure 7: Plot of state variables z for both the coupled circuits with $R_{12} = 17000$ (chaotic-chaotic initial conditions). Zoom is shown for both the regions of chaotic (box at the top) and more regular pseudosinusoidal oscillations (box at the bottom).

$$\frac{dy}{dt} = \frac{1}{C_2}\left(\frac{z-y}{R} + x\right), \tag{3b}$$

$$\frac{dz}{dt} = \frac{1}{C_1}\left(\frac{y-z}{R} - i_M\right), \tag{3c}$$

$$\frac{dw}{dt} = z, \tag{3d}$$

where x is the current through the inductor L, y and z represent the voltages across the capacitor C_2 and C_1, respectively, w is the magnetic flux and $i_M = W(\varphi) \cdot V_1$ is the current through the memristor.

Note that (3a)–(3c) are formally identical to ones reported in the literature for the Chua's circuit [58] with the only difference that the current of the diode is replaced by the current through the memristor. Moreover, due to the presence of a new equation for the magnetic flux (or for the charge in the case of charge-controlled memristor), the substitution of the Chua's diode with a memristor augments the dimension of the equation set describing the original circuit. To obtain chaotic dynamic, the circuit parameters are set to $L = 18\,\text{mH}$, $C_2 = 68\,\text{nF}$, $C_1 = 6.8\,\text{nF}$, and $R = 2000\,\Omega$ in original paper describing this circuit [57], and a chaotic attractor is found by numerical simulation of (3a)–(3d) starting from the following initial conditions: $x(0) = 0$, $y(0) = 0.11$, $z(0) = 0.11$, and $w(0) = 0$. In order to study the dynamics of the memristor-based Chua's circuits, the MATLAB function ode45 implementing an explicit 4th and 5th order Runge-Kutta formula based on the Dormand-Prince method [59] is used in this work.

A chaotic dynamics was also found for initial conditions [−24.33, −12480, −7294, 2.948]. Figure 2 shows a 3D projection of the attractor with corresponding time series of the signals.

As is well known, however, chaotic systems are very sensitive to the changes of the initial conditions and different initial values can generate totally different behavior. In order to describe the diverse dynamics of the system (3a)–(3d) produced to vary the initial conditions, the peaks of the flux $w(t)$ as a function of its initial values $w(0)$ was calculated for initial conditions [0, 23000, 1250, $w(0)$]. The resulting bifurcation diagram is shown in Figure 3 (peaks of $w(t)$ were recorded after transient).

Coexistence of multiple attractors in the phase space is evident, and a very interesting progression of the dynamics with varying $w(0)$ appears. For example, a scenario with Hopf-like bifurcations and period doubling bifurcations is evident between points a and b of Figure 3, with limit cycles of increasing period (a zoom-in image of this area is shown in the box at the top). For lower $w(0)$ values up to the point c, there is an area of fully developed chaos with Chua's spiral-type attractor (Figure 4). Windows of n-order limit cycles and trivial fixed points $(0, 0, 0, w = \text{const})$ corresponding to the damping of the system also appear.

Between positions d and e, the expansion of points indicates the birth of a double-scroll type attractor (such as that shown in Figure 2). Finally, the straight lines at lower values of $w(0)$ indicate the saturation of the systems to a period one orbit, with nonchaotic pseudosinusoidal oscillations of higher amplitude.

Therefore, in addition to the chaotic behaviour and depending on the initial conditions of the circuit, nonchaotic oscillations and damped oscillations are also identified for the system (3a)–(3d). In particular, for initial conditions [112.4047, 27015, 9360, −4.0542] and [−178.1619, −66031, −16762, 4.5430] the system produces nonchaotic and pseudosinusoidal oscillations, with a limit cycle of period 1 in the phase space (Figure 5). This dynamics corresponds to the saturation described above. For initial conditions [22, 10000, 0.15, 0.2] and [−20, −10000, 50000, −2] the circuit is damped, and a sink appears in the phase space. These values are just some of the initial conditions that have been considered in order to obtain a coarse characterization of the basins of attraction for the system (3a)–(3d). Further investigations are needed to adequately describe these basins of attraction but it is beyond the scope of the present work. However, the initial conditions indicated above produce the whole dynamic behaviors observed for the single circuit. They result in distant areas of the single circuit phase space and were used to simulate the coupling of circuits starting from significantly different initial conditions, as described in the following section.

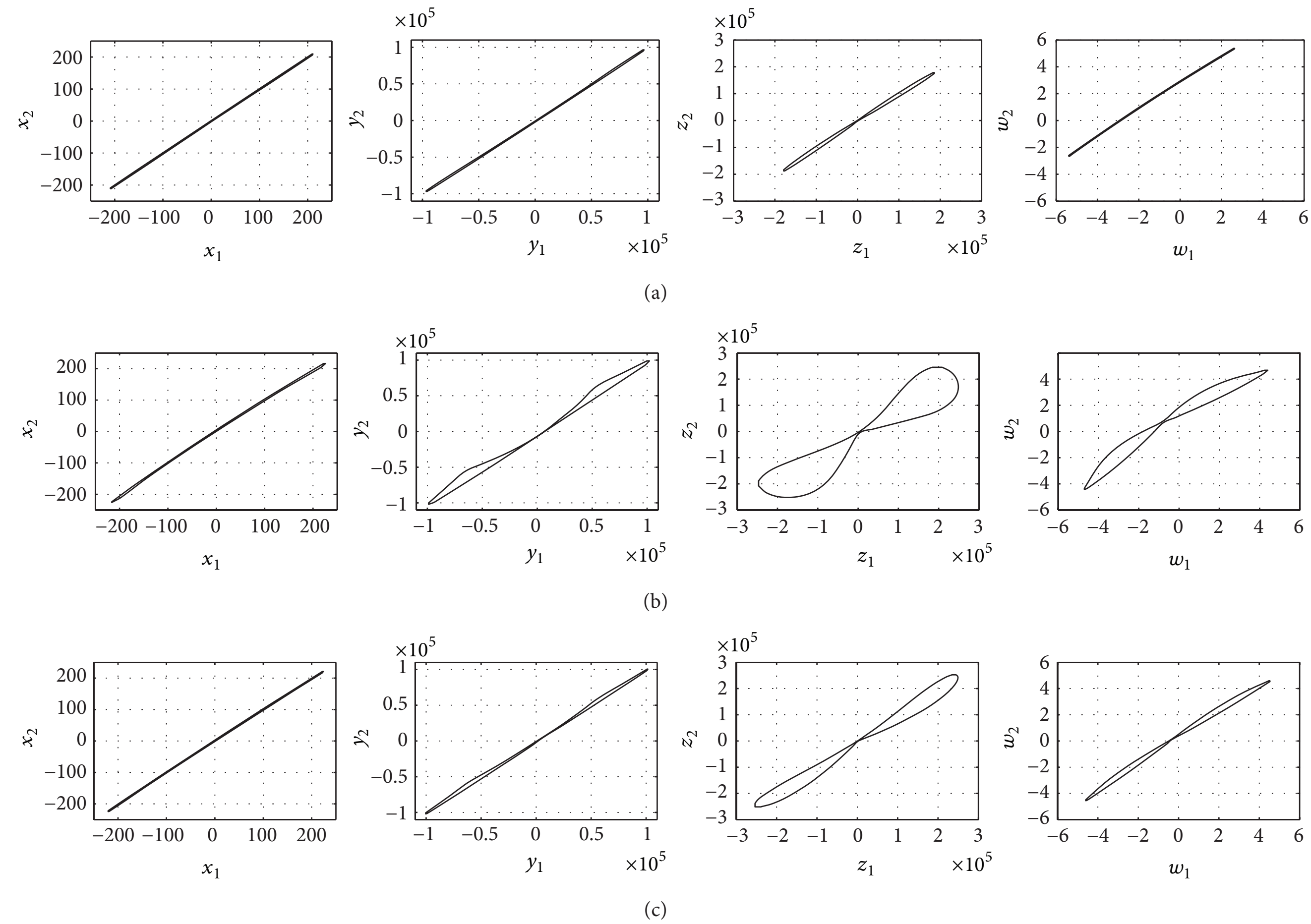

Figure 8: Phase portraits between corresponding signals of the two coupled circuits during the steady state of nonchaotic oscillation (C-C initial conditions) for different coupling strength. From top: $R_{12} = 100, 10000, 40000$.

3. The Coupling Scheme

In this study, two memristor-based Chua's circuits described above are mutually coupled through a resistor R_{12} as shown in Figure 6.

The equations describing the dynamic of the system are:

$$\frac{dx_1}{dt} = -\frac{y_1}{L}, \tag{4a}$$

$$\frac{dy_1}{dt} = \frac{1}{C_2}\left(\frac{z_1 - y_1}{R} + x_1\right), \tag{4b}$$

$$\frac{dz_1}{dt} = \frac{1}{C_1}\left(\frac{y_1 - z_1}{R} - \left(\frac{z_1 - z_2}{R_{12}}\right) - W(w_1)\cdot z_1\right), \tag{4c}$$

$$\frac{dx_2}{dt} = -\frac{y_2}{L}, \tag{4d}$$

$$\frac{dy_2}{dt} = \frac{1}{C_2}\left(\frac{z_2 - y_2}{R} + x_2\right), \tag{4e}$$

$$\frac{dz_2}{dt} = \frac{1}{C_1}\left(\frac{y_2 - z_2}{R} + \left(\frac{z_1 - z_2}{R_{12}}\right) - W(w_2)\cdot z_2\right), \tag{4f}$$

$$\frac{dw_1}{dt} = z_1, \tag{4g}$$

$$\frac{dw_2}{dt} = z_2, \tag{4h}$$

where symbols have the same meaning as in (3a)–(3d), and subscripts refer to the two circuits.

Accurate numerical integration of (4a)–(4h) was performed for different values of the coupling resistor R_{12} in order to investigate the occurrence of self-induced synchronization phenomena during the free evolution of the system. Since, depending on the initial conditions, the behavior of the single memristor-based circuit can be chaotic (C), oscillating with pseudosinusoidal (PS) dynamics, and damped (D); there are 6 qualitatively different choices for the initial conditions of the two coupled circuits: C-C, C-D, C-PS, D-D, D-PS, and PS-PS. All of these cases were examined using the initial conditions given above. The range of variation for the coupling resistor was initially set to $R_{12} \in \{0.1, 1.0, 2.0, 3.0, 4.0, 5.0, 6.0, 7.0, 8.0, 9.0, 10.0, 15.0, 20.0, 25.0, 30.0, 35.0, 40.0, 45.0, 50.0, 60.0, 70.0, 80.0, 90.0, 100.00\}\cdot 10^3$. Note that the presence of the resistor $R = 1000$ in the circuit fixes a natural length scale for the resistances, and the

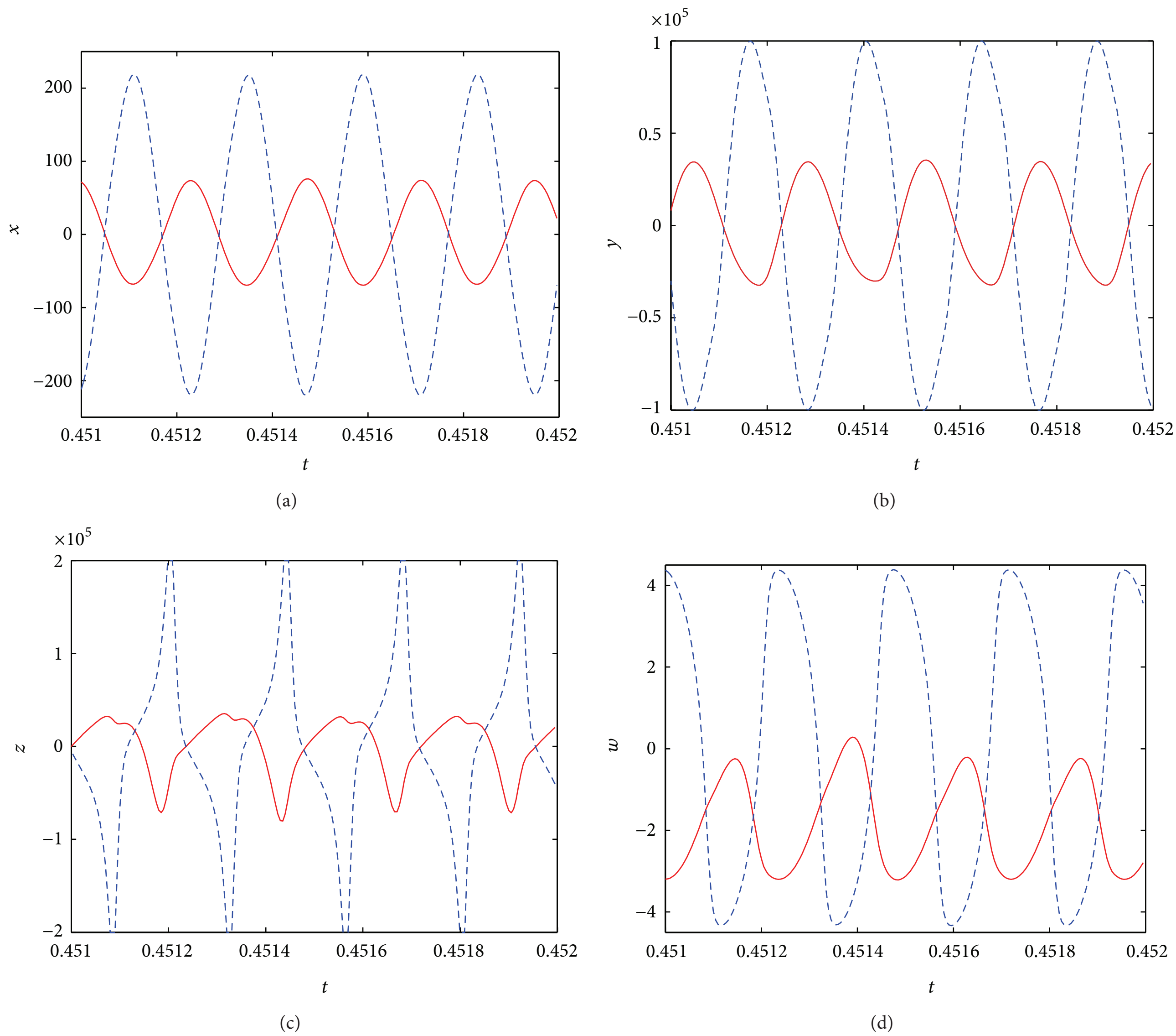

FIGURE 9: Pair of time series of the two mutually coupled circuits, for C-C initial conditions and $R_{12} = 20000$. Signals are out of phase with different amplitudes, and some kind of AS is observed.

investigated range for the coupling factor R_{12} correspond to $\sim 10^{-1}R \leq R_{12} \leq \sim 10^{2}R$, that is, a variation of a few orders of magnitude with respect to R. Numerical simulations were carried out for $t \in [0,1]$ s. Additional values of R_{12} and longer integration times were investigated when deemed necessary, as detailed below.

4. Simulation Results

The results obtained in the C-C and C-D cases qualitatively reproduce the entire phenomenology observed in all the simulations performed for this study, and only these two cases will be presented below in detail.

4.1. Chaotic-Chaotic (C-C) Initial Conditions. For high coupling (low R_{12}) nonchaotic synchronization occurs. In more details, for $R_{12} \in [100, 40000]$ and $R_{12} \neq 20000$, after an initial transient during which the two circuits oscillate in a chaotic and uncorrelated way, they reach a state of nonchaotic synchronization. In Figure 7 the time series of the variables y_1 and y_2 in the case of $R_{12} = 17000$ are depicted. The qualitative trend of other signals is similar to the presented one.

It is evident that an initial state of chaotic behavior exists, with a double-scroll type attractor such as that shown in Figure 2, followed by a situation in which the two circuits oscillate with larger amplitude in a pseudosinusoidal manner. In this latter case the trajectories of the two coupled circuits are limit cycles of order 1 in their respective phase space, as shown in Figure 4.

The existence of some kind of synchronization in this state of nonchaotic oscillation is evidenced by the appearance of well-defined curves in the phase portraits between

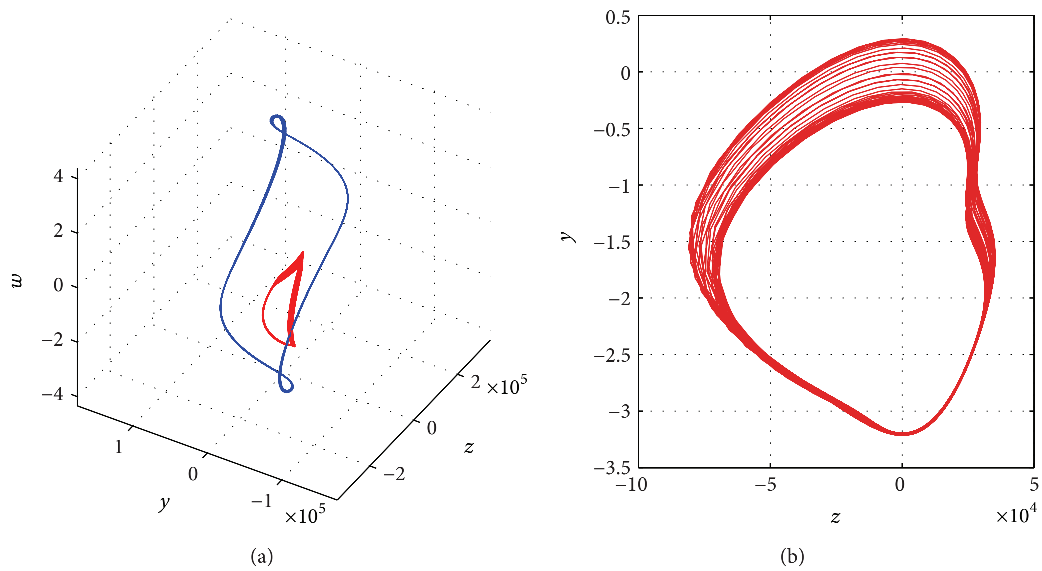

Figure 10: 3D projection (y, z, w) of the attractors (a) of the two coupled circuits for the case of C-C initial conditions and $R_{12} = 20000$. (b) 2D projection (y versus z) of the Chua's spiral type attractor is depicted.

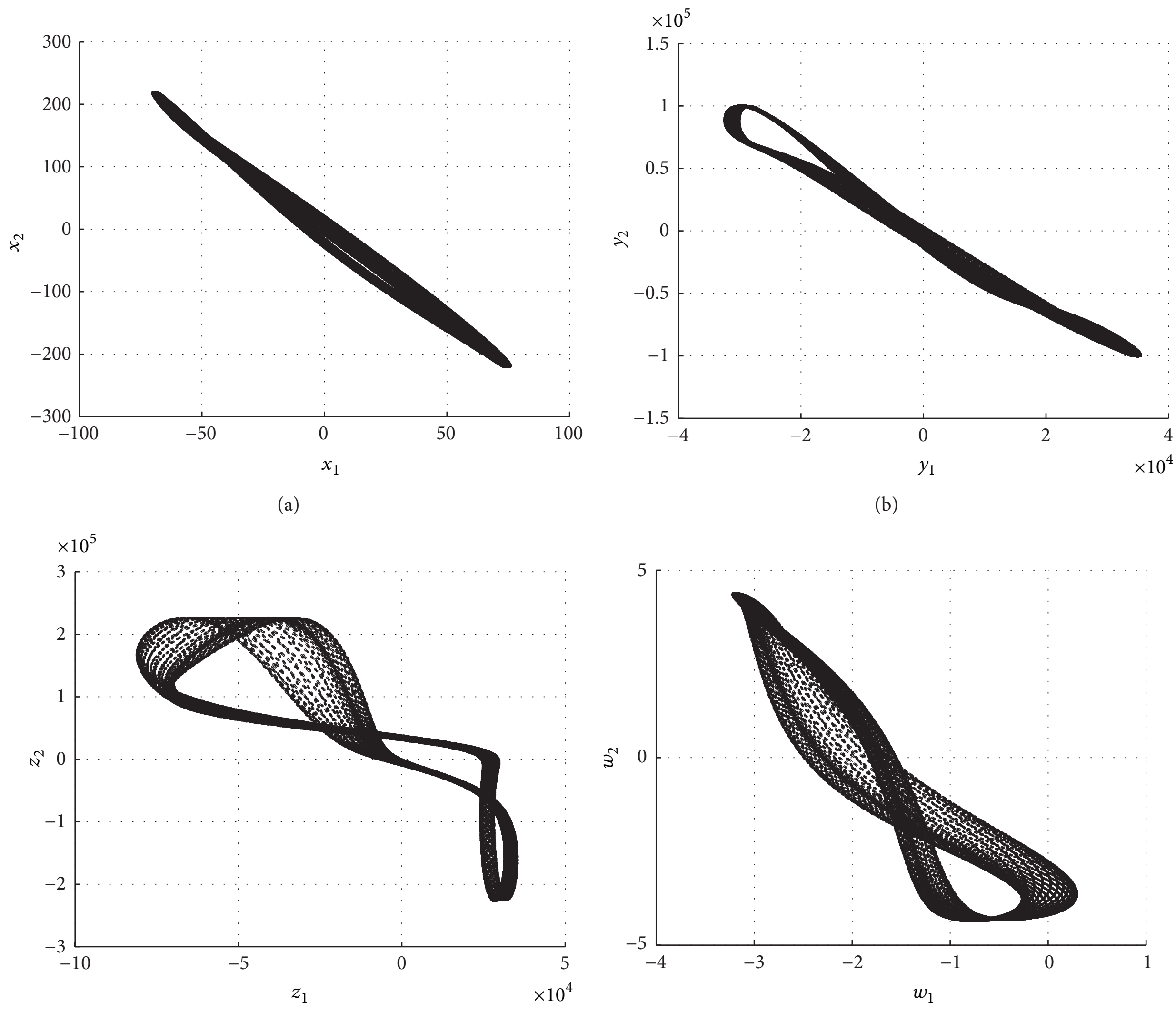

Figure 11: Phase diagrams during the steady state of the systems for $R_{12} = 20000$ and chaotic-chaotic initial conditions.

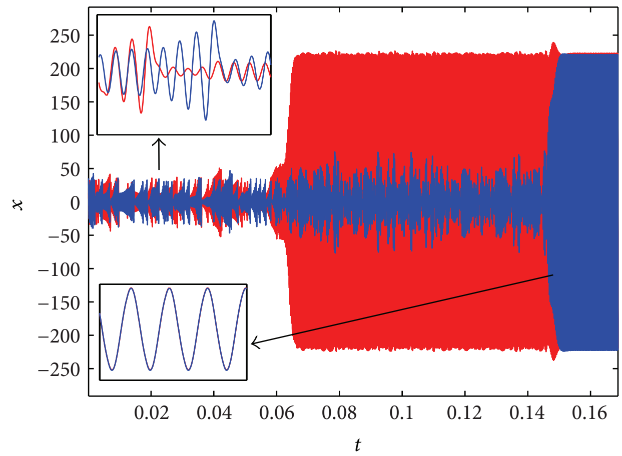

Figure 12: Plot of state variables x for both the coupled circuits with $R_{12} = 40000$ (C-C initial conditions). The duration of the chaotic and uncorrelated transient is different for the two circuits. Zoom is shown for the region of the first chaotic transient (box at the top) and for the nonchaotic synchronization final state (box at the bottom).

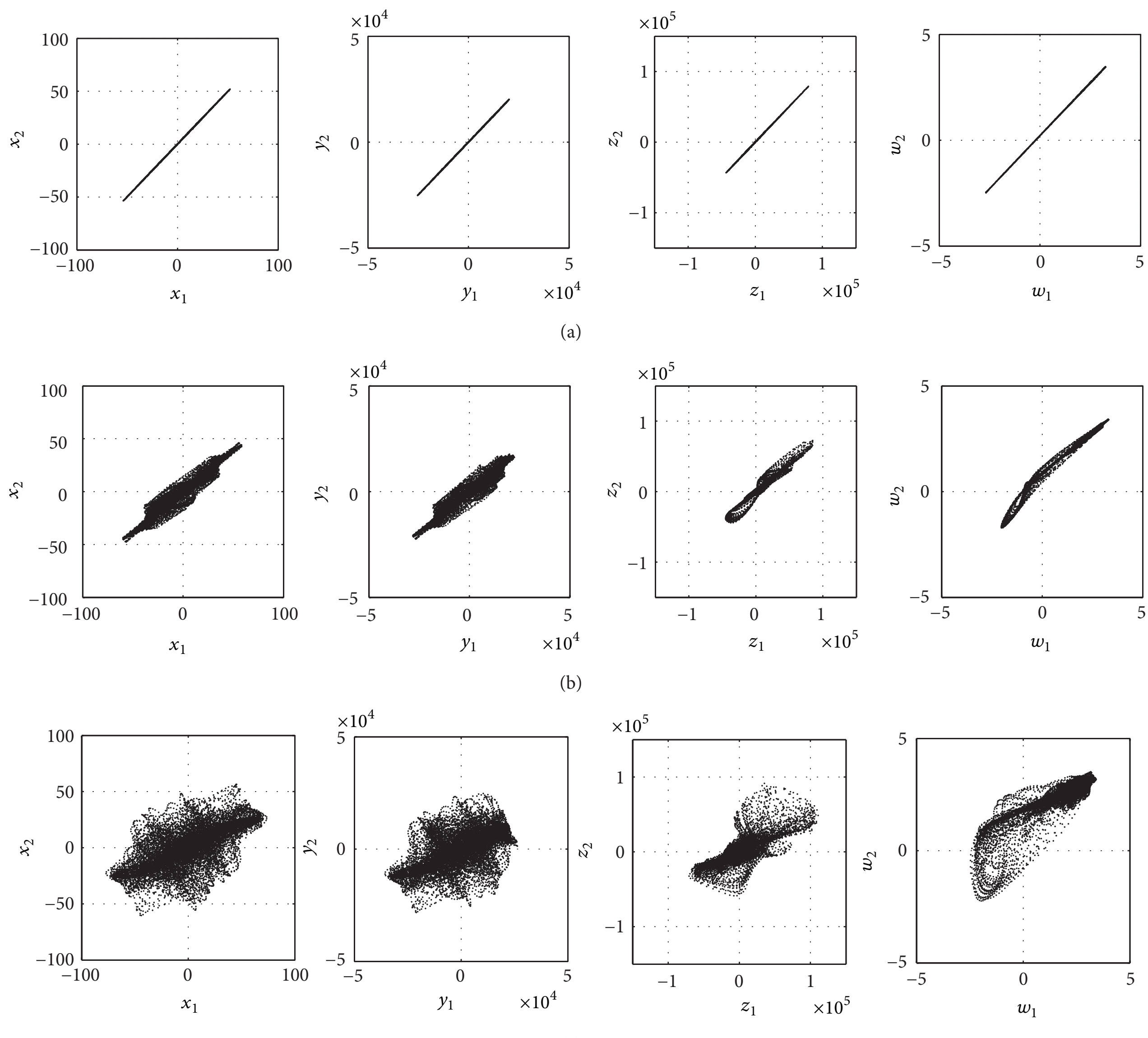

Figure 13: Phase diagrams during the chaotic oscillations of the two coupled circuits starting from chaotic-damped initial conditions. From top: $R_{12} = 100, 4000, 9000$.

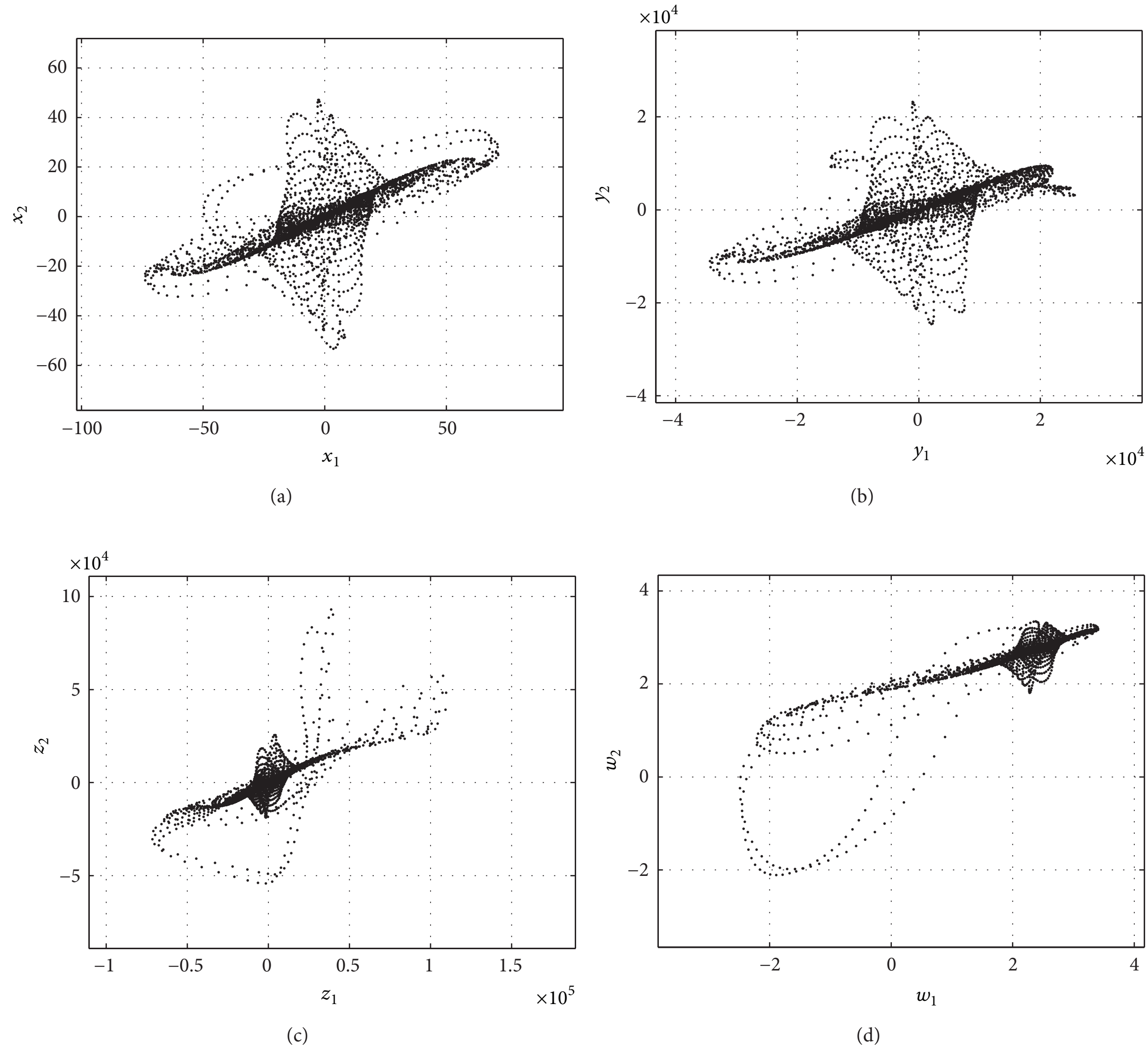

Figure 14: Phase diagrams for chaotic-chaotic initial conditions and $R_{12} = 9000$. The signals are considered on a time interval of 0.02 s.

corresponding signals of the two coupled circuits (Figure 8). In particular, for $R_{12} = 100$ the signals are practically coincident except for a constant bias for the flux, and a straight line appears in the phase diagrams (Figure 8(a)). For the other investigated values of R_{12}, the curves in the phase diagrams assume the form of a hysteresis-like loop with a single pinch (Figures 8(b) and 8(c))). It is worthy to note that during this steady state of pseudosinusoidal oscillation, the corresponding signals present a periodic phase shift. The amplitude difference between the signals and the initial phase shift change as R_{12} varies, and this determines the different aspect of the phase diagrams shown in Figure 8.

For $R_{12} = 20000$ the behavior of the system is quite different. After a chaotic and uncorrelated transient, the two coupled circuits achieve a steady state in which the corresponding signals are completely out of phase (Figure 9). Some kind of antisynchronization [60] (AS) with significantly different amplitudes is observed in this case. Moreover, as shown in Figure 10, phase trajectories of the two systems evolve on different attractors; in particular, the circuit 2 is on a Chua's spiral-type attractor.

The phase diagrams are now more complex (Figure 11), but they still indicate the presence of some kind of synchronization [53].

The steady state behavior for $R_{12} = 20000$ with the signals out of phase seems to be peculiar. Indeed, simulations carried out for $R_{12} \in \{19.1, 19.2, 19.5, 19.9, 19.999,$ c$20.001, 20.01, 20.1, 20.2\}\cdot 10^3$ have produced results in accordance with that previously reported for $R_{12} \leq 40000$ and $R_{12} \neq 20000$ (in-phase pseudosinusoidal oscillations).

For $R_{12} = 40000$, the system presents a new feature: the duration of the chaotic and uncorrelated transient is different for the two coupled circuits (Figure 12). Only after both

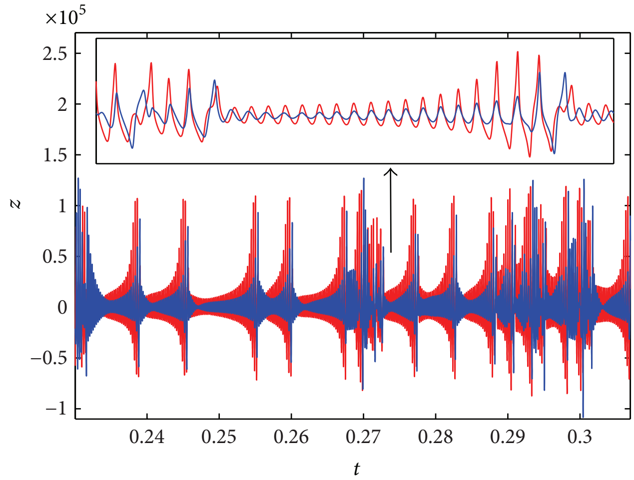

FIGURE 15: Plot of state variables z for both the coupled circuits at $R_{12} = 9000$ for C-D initial conditions. The signals pass through a progression of deconstruction and recomposition of the state of phase-synchronization.

circuits enter into high-amplitude pseudosinusoidal oscillation synchronization occurs, with characteristics similar to cases of $R_{12} \neq 20000$. In particular, the attractors of the two circuits are limit cycles of order 1.

Finally, for $R_{12} \geq 45000$ the two circuits are practically uncoupled and the respective signals still remain uncorrelated. In more details, after a transient in which both circuits oscillate chaotically, only one circuit begins to oscillate in nonchaotic way with pseudosinusoidal oscillations and greater amplitude for $R_{12} = 45000$. This uncorrelated coexistence of order and chaos remained unchanged in simulations of the dynamics of the system up to 80 s. For $R_{12} \geq 50000$ the two circuits remain in chaotic and uncorrelated oscillation.

4.2. Chaotic-Damped (C-D) Initial Conditions. Similarly as discussed above, a synchronization state with pseudosinusoidal oscillations is also observed in this case for low coupling. Moreover, a situation of chaotic oscillations with strong correlation between signals is also found at high coupling for $R_{12} \leq 9000$.

In more detail, for $R_{12} = 100$ (Figure 13(a)) the phase portraits indicate a condition of CS, but as R_{12} increases the correlation between the signals rapidly decreases (Figures 13(b) and 13(c)). In effect, the phase diagrams contain points whose dispersion around the diagonal depends on the value of R_{12}. For the lowest investigated value of R_{12}, trajectories in the phase portraits remain most of the time on the diagonal, and the synchronization is easy to recognize. As R_{12} increases, the duration of periods of desynchronization, that is, the amount of points far from the diagonal, increases and it masks possible "structures" indicating correlation.

In order to highlight this behavior, in Figure 14 the phase diagrams are plotted for a time interval of 0.02 s with $R_{12} = 9000$. Despite the cloud-like shape of the corresponding phase diagram in Figure 13(c), from Figure 14 it is clear that the system passes through a sequence of phase-synchronized states. In effect, observing the signals of the two circuits (Figure 15) it is possible to note a rapid alternation of situations in which the signals are uncorrelated and situations in which the signals oscillate in phase, and a deconstruction and recomposition of the state of phase synchronization happen.

For $10000 \leq R_{12} \leq 20000$ the two circuits reach a state of nonchaotic synchronization with pseudosinusoidal oscillations. More precisely, as reported in Figure 16(a) for $R_{12} = 10000$, after a chaotic transient the circuits have a behavior similar to that shown in Figure 7, with high-amplitude pseudosinusoidal oscillations that result strongly correlated. The attractors of the synchronized circuit are limit cycles of order 1 (such as that shown in Figure 5).

For $R_{12} \in [15000, 20000]$ the chaotic transient disappears and systems immediately synchronize with nonsaturated oscillations (phase diagrams depicted in Figures 16(b) and 16(c)). The attractors are limit cycles of periods 1 and 2, respectively, which result similar to the attractors displayed by the single system (3a)–(3d) during the period doubling bifurcations described in section 2. The amplitude of the oscillations for the circuit starting from damping initial condition is an order of magnitude lower than the other circuit.

Finally, for $R_{12} \geq 25000$ both the two systems remain in chaotic oscillation at different amplitudes evolving on Chua's spiral like attractors. The phase portraits for this case, shown in Figure 17, indicate very weak or null correlation. Unlike what happens for $R_{12} \leq 9000$, also at smaller time scale, coherent substructures do not emerge in the phase diagrams.

5. Conclusion

In this paper the problem of spontaneous self-synchronization of two mutually coupled memristor-based Chua's circuits is investigated via numerical simulations. The great sensitivity of the single circuit on initial conditions was here investigated by means of a bifurcations diagram for the maxima of the flux $w(t)$ as a function of its initial values $w(0)$. A complex progression of the dynamics with varying initial conditions is evident. Beside chaotic (C) dynamics, pseudosinusoidal (PS) oscillations, and damped (D) oscillations were also identified for the single memristor based circuit.

A diffusive coupling between two of these circuits was realized with a resistor R_{12} and accurate numerical simulations were performed for various values of the coupling resistor and for different initial conditions. Synchronization states were identified by the appearance of patterns in the phase portraits of the system which indicate correlation between the signals of the two circuits.

It was found that, depending on the initial conditions and on the coupling strength, both nonchaotic and chaotic synchronization is possible for the coupled circuits. Nonchaotic synchronization with positive correlation between signals seems to be the most frequent situation for the investigated system, and it was observed for all the initial conditions

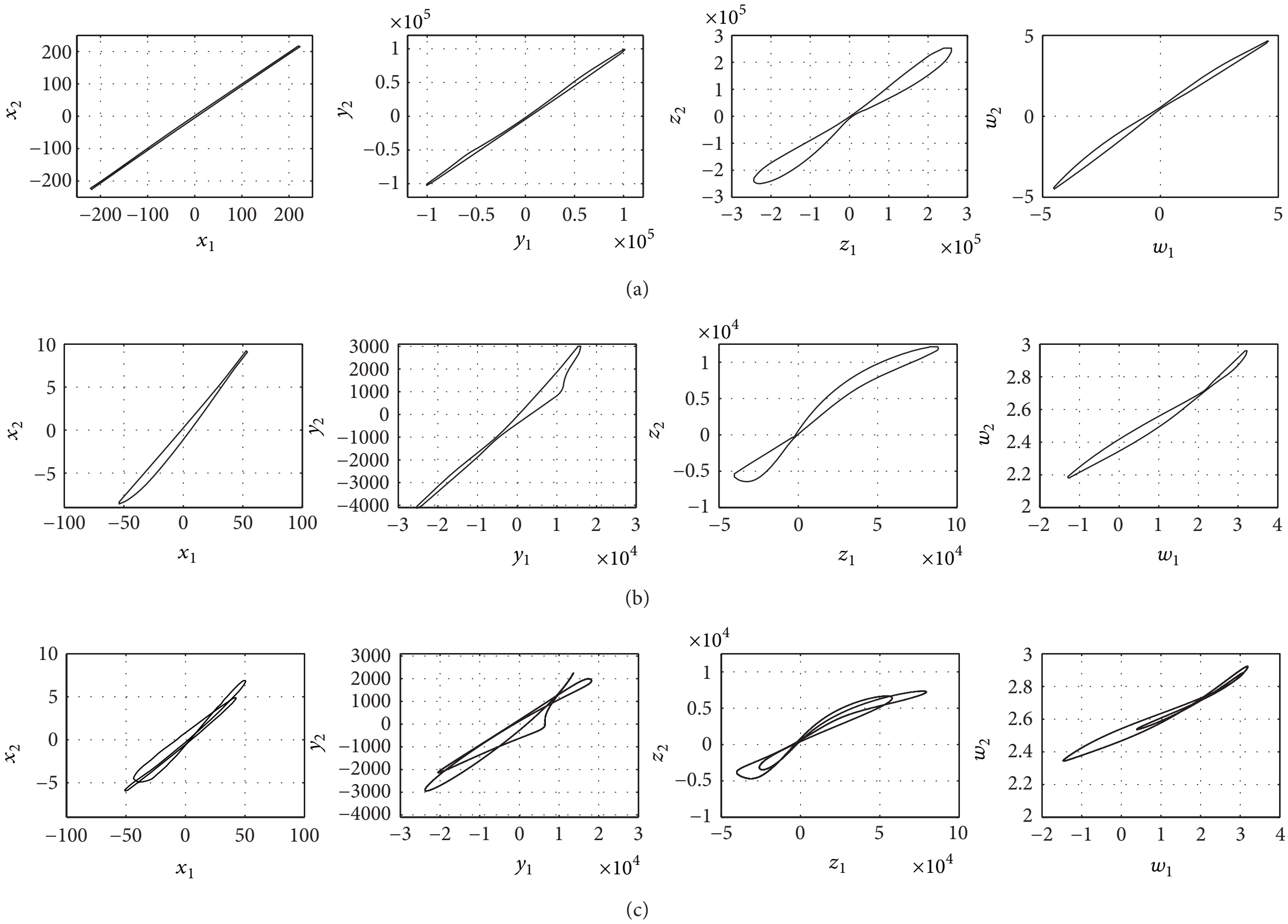

FIGURE 16: Phase diagram during the pseudosinusoidal oscillations of the two coupled circuits starting from chaotic-damped initial conditions. From top: R_{12} = 10000, 15000, 20000.

examined and for a wide range of R_{12} values. In this case the circuits exhibit pseudosinusoidal waveform oscillations with a small periodic phase shift between corresponding signals of the two coupled circuits. This results in curves forming a hysteresis-like loop in the phase portraits.

Chaotic synchronization was found only for C-D initial conditions at high coupling (small values of R_{12}) and it is produced by a rapid succession of uncorrelated and phase-correlated oscillations. Phase portraits show points scattered around the diagonal line, with positive correlation. The duration of the period during which the signals are uncorrelated increases with R_{12} and more smeared phase portraits occur.

With respect to the whole numerical results obtained in this study, a peculiar situation was detected for C-C initial conditions at $R_{12} = 9000$. In this case the oscillations of the two circuits are completely out of phase and with significantly different amplitudes. Phase portraits show complex patterns with negative correlation that clearly indicate some kind of synchronization.

Moreover, numerical integrations showed that transient chaos, already reported in literature for single memristor-based systems, also is possible for the coupled circuits examined in this work. In fact, chaotic and uncorrelated oscillations may precede for a significant time the onset of pseudosinusoidal synchronization.

Finally, computer simulations also indicate the possibility of uncorrelated coexistence of chaos and order. In particular, this situation can be a transient state which precedes nonchaotic synchronization or, for low coupling strength, a stationary state of the coupled circuits.

Therefore, the two mutually coupled memristor-based chaotic circuits studied in this work display a complex dynamic with a great variety of both chaotic and nonchaotic synchronisms. A possible interpretation for this can be that, due to the presence of the memory effect of the memristor that results in different memductances values for the circuits, the two considered dynamical systems are not completely identical, and various kinds of synchronization are expected. In effect, if complete synchronization appears only at high coupling strength, some form of phase synchronization or generalized synchronization seems to be more suitable for interpreting most of the numerical results obtained in this work, which could provide new insights for further study

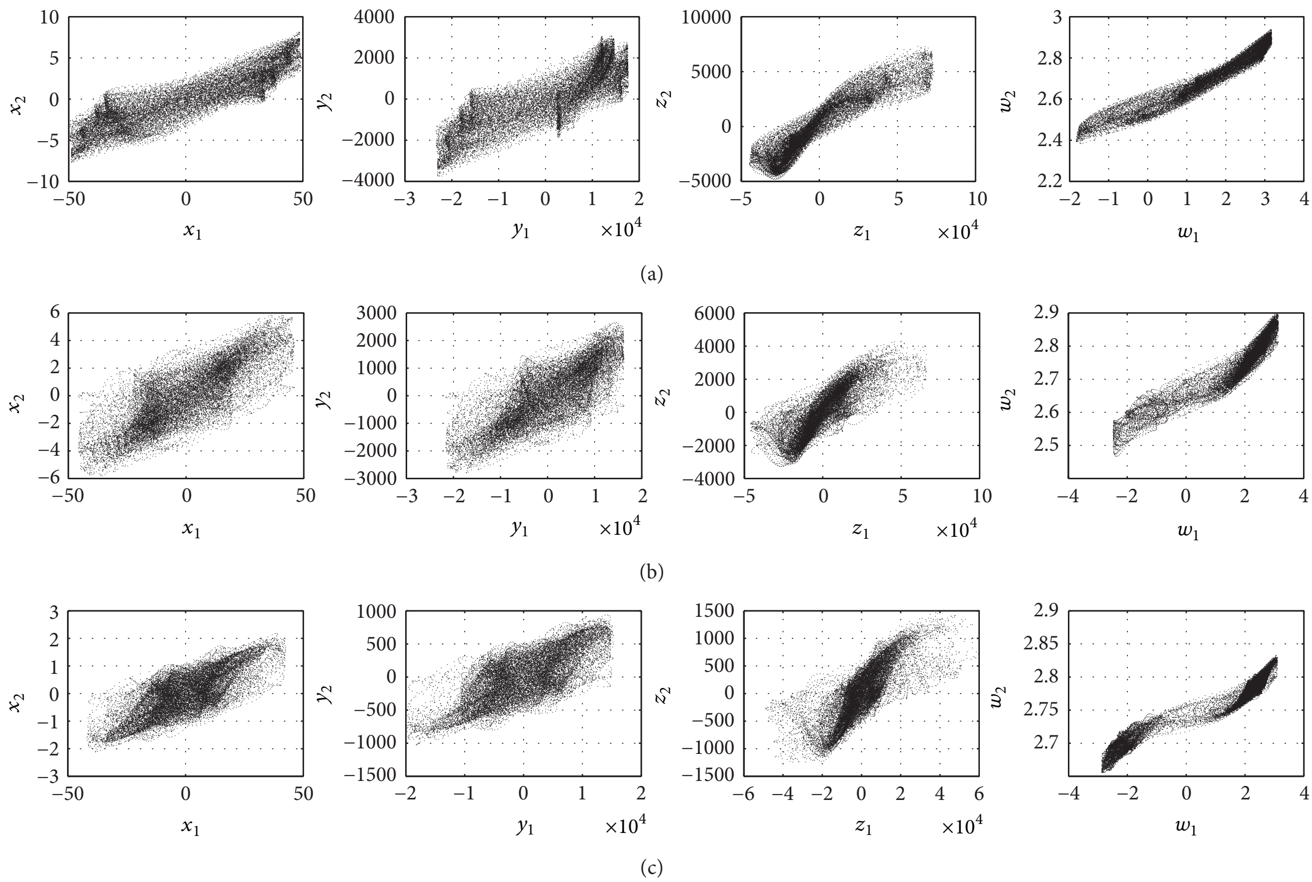

FIGURE 17: Phase diagram during the chaotic oscillations of the two circuits starting from chaotic-damped initial conditions and coupled with high values of R_{12}. From top: $R_{12} = 25000, 40000, 100000$.

to better understand the spontaneous dynamic of coupled memristor-based chaotic systems. In particular, although the results presented here are not directly generalizable to the case of multiple mutually coupled oscillators, because emergent phenomena can occur in the case of collective dynamics, they may be a useful reference for studying multiple systems. For example, the spontaneous dynamics of multiple memristor-based Chua's circuits diffusively coupled in a ring geometry has been investigated in our recent paper [61]. In addition to chaotic and nonchaotic synchronization, also emerging chaotic steady waves and quasi-periodic traveling waves along the ring have been observed.

Conflict of Interests

The authors declare that they have no conflict of interests regarding the publication of this paper.

Acknowledgment

This work was cofunded by the European Commission, FSE, Regione Calabria (Italy).

References

[1] E. Bilotta, G. Di Blasi, F. Stranges, and P. Pantano, "A gallery of Chua attractors—part V," *International Journal of Bifurcation and Chaos*, vol. 17, no. 5, pp. 1383–1511, 2007.

[2] E. Bilotta, G. Di Blasi, F. Stranges, and P. Pantano, "A gallery of Chua attractors—part VI," *International Journal of Bifurcation and Chaos*, vol. 17, no. 6, pp. 1801–1910, 2007.

[3] E. Bilotta and P. Pantano, "Emergent patterning phenomena in 2D cellular automata," *Artificial Life*, vol. 11, no. 3, pp. 339–362, 2005.

[4] E. Bilotta and P. Pantano, "Synthetic harmonies: recent results," *Leonardo Journal*, vol. 35, pp. 35–42, 2002.

[5] E. Bilotta, E. Bossio, and P. Pantano, "Chaos at school: Chua's circuit for students in junior and senior high school," *International Journal of Bifurcation and Chaos*, vol. 20, no. 1, pp. 1–28, 2010.

[6] E. Bilotta, P. Pantano, E. Cupellini, and C. Rizzuti, "Evolutionary methods for melodic sequences generation from non-linear dynamic systems," in *Applications of Evolutionary Computing*, vol. 4448 of *Lecture Notes in Computer Science*, pp. 585–592, 2007.

[7] E. Bilotta, P. Pantano, and S. Vena, "Artificial micro-worlds part I: a new approach for studying life-like phenomena,"

International Journal of Bifurcation and Chaos, vol. 21, no. 2, pp. 373–398, 2011.

[8] E. Bilotta and P. Pantano, "Artificial micro-worlds part II: cellular automata growth dynamics," *International Journal of Bifurcation and Chaos*, vol. 21, no. 3, pp. 619–645, 2011.

[9] L. M. Pecora, T. L. Carroll, G. A. Johnson, D. J. Mar, and J. F. Heagy, "Fundamentals of synchronization in chaotic systems, concepts, and applications," *Chaos*, vol. 7, no. 4, pp. 520–543, 1997.

[10] S. Boccaletti, J. Kurths, G. Osipov, D. L. Valladares, and C. S. Zhou, "The synchronization of chaotic systems," *Physics Report*, vol. 366, no. 1-2, pp. 1–101, 2002.

[11] C. Wu and L. O. Chua, "A simple way to synchronize chaotic systems with applications to secure communication systems," *International Journal of Bifurcation and Chaos*, vol. 3, pp. 1619–1627, 1993.

[12] A.-V. Diaconu and K. Loukhaoukha, "An improved secure image encryption algorithm based on Rubik's Cube principle and digital chaotic cipher," *Mathematical Problems in Engineering*, vol. 2013, Article ID 848392, 10 pages, 2013.

[13] J. Sun, Y. Shen, Q. Yin, and C. Xu, "Compound synchronization of four memristor chaotic oscillator systems and secure communication," *Chaos*, vol. 23, Article ID 013140, 2013.

[14] E. Mosekilde, Y. Maistrenko, and D. Postnov, *Chaotic Synchronization: Applications to Living Systems*, World Scientific, Hackensack, NJ, USA, 2002.

[15] L. M. Pecora and T. L. Carroll, "Synchronization in chaotic systems," *Physical Review Letters*, vol. 64, no. 8, pp. 821–824, 1990.

[16] G. Chen and X. Yu, *Chaos Control: Theory and Applications*, Springer, Heidelberg, Germany, 2003.

[17] T. Youssef, M. Chadli, H. R. Karimi, and M. Zelmat, "Chaos synchronization based on unknown input proportional multiple-integral fuzzy observer," *Abstract and Applied Analysis*, vol. 2013, Article ID 670878, 11 pages, 2013.

[18] B. Wang, P. Shi, H. R. Karimi, Y. Song, and J. Wang, "Robust synchronization of a hyper-chaotic system with disturbance input," *Nonlinear Analysis: Real World Applications*, vol. 14, pp. 1487–1495, 2013.

[19] H. R. Karimi, "A sliding mode approach to H∞ synchronization of masterslave time-delay systems with Markovian jumping parameters and nonlinear uncertainties," *Journal of the Franklin Institute*, vol. 349, no. 4, pp. 1480–1496, 2012.

[20] H. R. Karimi and H. Gao, "New delay-dependent exponential H∞ synchronization for uncertain neural networks with mixed time delays," *IEEE Transactions on Systems, Man, and Cybernetics B: Cybernetics*, vol. 40, no. 1, pp. 173–185, 2010.

[21] H. R. Karimi and P. Maass, "Delay-range-dependent exponential H∞ synchronization of a class of delayed neural networks," *Chaos, Solitons and Fractals*, vol. 41, no. 3, pp. 1125–1135, 2009.

[22] Y. Yu and S. Zhang, "The synchronization of linearly bidirectional coupled chaotic systems," *Chaos, Solitons and Fractals*, vol. 22, no. 1, pp. 189–197, 2004.

[23] S. Wen, Z. Zeng, and T. Huang, "Adaptive synchronization of memristor-based Chua's circuits," *Physics Letters A*, vol. 376, pp. 2775–2780, 2012.

[24] S. Wen, Z. Zeng, T. Huang, and Y. Chen, "Fuzzy modeling and synchronization of different memristor-based chaotic circuits," *Physics Letters A*, vol. 337, pp. 2016–2021, 2013.

[25] S. C. Mansubia, A. S. Mikhailov, and D. H. Zanette, *Emergence of Dynamical Order: Synchronization Phenomena in Complex Systems*, World Scientific, Singapore, 2004.

[26] J. K. Hale, "Diffusive coupling, dissipation, and synchronization," *Journal of Dynamics and Differential Equations*, vol. 9, no. 1, pp. 1–52, 1997.

[27] A. Buscarino, L. Fortuna, M. Frasca, and G. Sciuto, "Chua's circuits synchronization with diffusive coupling: new results," *International Journal of Bifurcation and Chaos*, vol. 19, no. 9, pp. 3101–3107, 2009.

[28] L. Chua, "Memristor-the missing circuit element," *IEEE Trans Circuit Theory*, vol. 18, no. 5, pp. 507–519, 1971.

[29] D. B. Strukov, G. S. Snider, D. R. Stewart, and R. S. Williams, "The missing memristor found," *Nature*, vol. 453, pp. 80–83, 2008.

[30] Y. N. Joglekar and S. J. Wolf, "The elusive memristor: properties of basic electrical circuits," *European Journal of Physics*, vol. 30, no. 4, pp. 661–675, 2009.

[31] O. Kavehei, A. Iqbal, Y. S. Kim, K. Eshraghian, S. F. Al-Sarawi, and D. Abbott, "The fourth element: characteristics, modelling and electromagnetic theory of the memristor," *Proceedings of the Royal Society A: Mathematical, Physical and Engineering Sciences*, vol. 466, no. 2120, pp. 2175–2202, 2010.

[32] Y. Ho, G. M. Huang, and P. Li, "Dynamical properties and design analysis for nonvolatile memristor memories," *IEEE Transactions on Circuits and Systems I: Regular Papers*, vol. 58, no. 4, pp. 724–736, 2011.

[33] F. Merrikh-Bayat and S. B. Shouraki, "Memristor-based circuits for performing basic arithmetic operations," in *Proceedings of the 1st World Conference on Information Technology (WCIT '10)*, pp. 128–132, October 2010.

[34] S. Shin, K. Kim, and S.-M. Kang, "Memristor applications for programmable analog ICs," *IEEE Transactions on Nanotechnology*, vol. 10, no. 2, pp. 266–274, 2011.

[35] Y. V. Pershin, S. la Fontaine, and M. di Ventra, "Memristive model of amoeba learning," *Physical Review E*, vol. 80, Article ID 021926, 2009.

[36] T. Chang, Y. Yang, and W. Lu, "Building neuromorphic circuits with memristive devices," *IEEE Circuits and Systems Magazine*, vol. 13, no. 2, pp. 56–73, 2013.

[37] S. H. Jo, T. Chang, I. Ebong, B. B. Bhadviya, P. Mazumder, and W. Lu, "Nanoscale memristor device as synapse in neuromorphic systems," *Nano Letters*, vol. 10, no. 4, pp. 1297–1301, 2010.

[38] L. Wang, M. Duan, and S. Duan, "Memristive perceptron for combinational logic classification," *Mathematical Problems in Engineering*, vol. 2013, Article ID 625790, 7 pages, 2013.

[39] M. Itoh and L. O. Chua, "Memristor oscillators," *International Journal of Bifurcation and Chaos*, vol. 18, no. 11, pp. 3183–3206, 2008.

[40] B. Muthuswamy and P. P. Kokate, "Memristor-based chaotic circuits," *IETE Technical Review*, vol. 26, no. 6, pp. 417–429, 2009.

[41] B. Muthuswamy and L. O. Chua, "Simplest chaotic circuit," *International Journal of Bifurcation and Chaos*, vol. 20, no. 5, pp. 1567–1580, 2010.

[42] M. Messias, C. Nespoli, and V. A. Botta, "Hopf bifurcation from lines of equilibria without parameters in memristor oscillators," *International Journal of Bifurcation and Chaos*, vol. 20, no. 2, pp. 437–450, 2010.

[43] B. Bao, Z. Ma, J. Xu, Z. Liu, and Q. Xu, "A simple memristor chaotic circuit with complex dynamics," *International Journal of Bifurcation and Chaos*, vol. 21, no. 9, pp. 2629–2645, 2011.

[44] F. Corinto, A. Ascoli, and M. Gilli, "Nonlinear dynamics of memristor oscillators," *IEEE Transactions on Circuits and Systems I: Regular Papers*, vol. 58, no. 6, pp. 1323–1336, 2011.

[45] B.-C. Bao, Z. Liu, and J.-P. Xu, "Transient chaos in smooth memristor oscillator," *Chinese Physics B*, vol. 19, no. 3, Article ID 030510, 2010.

[46] B.-C. Bao, J.-P. Xu, and Z. Liu, "Initial state dependent dynamical behaviors in a memristor based chaotic circuit," *Chinese Physics Letters*, vol. 27, no. 7, Article ID 070504, 2010.

[47] C. K. Volos, I. M. Kyprianidis, I. N. Stouboulos, and C. Cepiscă, "Complex dynamics of a memristor based Chua's canonical circuit," in *Proceedings of the 15th Conference on Communications and Information Technology (CIT '11)*, pp. 111–116, July 2011.

[48] K. Pyragas, "Weak and strong synchronization of chaos," *Physical Review E—Statistical Physics, Plasmas, Fluids, and Related Interdisciplinary Topics*, vol. 54, no. 5, pp. R4508–R4511, 1996.

[49] V. C. Anishchenko, T. E. Vadivasova, V. V. Astakhov, O. V. Sosnovtseva, C. W. Wu, and L. O. Chua, "Dynamics of two coupled Chua's circuits," *International Journal of Bifurcation and Chaos*, vol. 5, pp. 1677–1699, 1995.

[50] A. Pikovsky, M. Rosenblum, and J. Kurths, "Phase synchronization in regular and chaotic systems," *International Journal of Bifurcation and Chaos in Applied Sciences and Engineering*, vol. 10, no. 10, pp. 2291–2305, 2000.

[51] M. G. Rosenblum, A. S. Pikovsky, and J. Kurths, "From phase to lag synchronization in coupled chaotic oscillators," *Physical Review Letters*, vol. 78, no. 22, pp. 4193–4196, 1997.

[52] L. Qun, P. Hai-Peng, X. Ling-Yu, and Y. Xian, "Lag synchronization of coupled multidelay systems," *Mathematical Problems in Engineering*, vol. 2012, Article ID 106830, 9 pages, 2012.

[53] A. M. dos Santos, S. R. Lopes, and R. L. Viana, "Rhythm synchronization and chaotic modulation of coupled Van der Pol oscillators in a model for the heartbeat," *Physica A: Statistical Mechanics and its Applications*, vol. 338, no. 3-4, pp. 335–355, 2004.

[54] J. Yang and G. Hu, "Three types of generalized synchronization," *Physics Letters A: General, Atomic and Solid State Physics*, vol. 361, no. 4-5, pp. 332–335, 2007.

[55] N. F. Rulkov, M. M. Sushchik, L. S. Tsimring, and H. D. I. Abarbanel, "Generalized synchronization of chaos in directionally coupled chaotic systems," *Physical Review E*, vol. 51, no. 2, pp. 980–994, 1995.

[56] L. Kocarev and U. Parlitz, "Generalized synchronization, predictability, and equivalence of unidirectionally coupled dynamical systems," *Physical Review Letters*, vol. 76, no. 11, pp. 1816–1819, 1996.

[57] B. Muthuswamy, "Implementing memristor based chaotic circuits," *International Journal of Bifurcation and Chaos*, vol. 20, no. 5, pp. 1335–1350, 2010.

[58] T. Matsumoto, "A chaotic attractor from Chua's circuit," *IEEE Transactions on Circuits and Systems*, vol. 31, no. 12, pp. 1055–1058, 1984.

[59] J. R. Dormand and P. J. Prince, "A family of embedded Runge-Kutta formulae," *Journal of Computational and Applied Mathematics*, vol. 6, no. 1, pp. 19–26, 1980.

[60] C. Li, Q. Chen, and T. Huang, "Coexistence of anti-phase and complete synchronization in coupled chen system via a single variable," *Chaos, Solitons and Fractals*, vol. 38, no. 2, pp. 461–464, 2008.

[61] E. Bilotta, F. Chiaravalloti, and P. Pantano, "Synchronization and waves in a ring of diffusively coupled memristor-based Chua's circuits," *Acta Applicandae Mathematicae*. In press.